The Journal of Experimental Biology 205, 3669–3677 (2002)
Printed in Great Britain © The Company of Biologists Limited 2002
JEB4273

Hovering flight mechanics of neotropical flower bats (Phyllostomidae: Glossophaginae) in normodense and hypodense gas mixtures

Robert Dudley[1,2,*] and York Winter[3]

[1]*Section of Integrative Biology, University of Texas at Austin, Austin, TX 78712, USA,* [2]*Smithsonian Tropical Research Institute, PO Box 2072, Balboa, Republic of Panama* and [3]*Department Biologie, Universität München, Luisenstrasse 14, 80333 München, Germany*

*Author for correspondence (e-mail: r_dudley@utxvms.cc.utexas.edu)

Accepted 11 September 2002

Summary

Existing estimates of flight energetics in glossophagine flower bats, the heaviest hovering vertebrate taxon, suggest disproportionately high expenditure of mechanical power. We determined wingbeat kinematics and mechanical power expenditure for one of the largest flower bats (*Leptonycteris curasoae* Martinez and Villa) during hovering flight in normodense and hypodense gas mixtures. Additional experiments examined the effects of supplemental oxygen availability on maximum flight performance. Bats failed to sustain hovering flight at normoxic air densities averaging 63% that of normodense air. Kinematic responses to hypodense aerodynamic challenge involved increases in wing positional angles and in total stroke amplitude; wingbeat frequency was unchanged. At near-failure air densities, total power expenditure assuming perfect elastic energy storage was 17–42% greater than that for hovering in normodense air, depending on the assumed value for the profile drag coefficient. Assuming a flight muscle ratio of 26%, the associated muscle-mass-specific power output at the point of near-failure varied between 90.8 W kg^{-1} (profile drag coefficient of 0.02) to 175.6 W kg^{-1} (profile drag coefficient of 0.2). Hyperoxia did not enhance hovering performance in hypodense air, and, with the exception of a small increase (10%) in stroke plane angle, yielded no significant change in any of the kinematic parameters studied. Revised energetic estimates suggest that mechanical power expenditure of hovering glossophagines is comparable with that in slow forward flight.

Key words: aerodynamics, bat, density, flight, glossophagine, hovering, hyperoxia, *Leptonycteris curasoae*, power.

Introduction

Glossophagine phyllostomid bats, commonly known as flower bats, range in mass up to 32 g and are the largest vertebrates capable of sustaining hovering flight. Although hovering duration in glossophagines is typically <1 s, hovering bouts can be much longer under experimental conditions and may last up to 17 s (see Voigt and Winter, 1999). Hovering in flower bats is associated with a partial supination of distal wing regions that yields vertically oriented lift during the upstroke (von Helversen, 1986). This kinematic feature distinguishes glossophagines from other bird and bat taxa that hover only transiently and use downstroke forces alone to offset body mass (Norberg, 1990). As in hummingbirds, the aerodynamic capacity of glossophagines to hover is associated with a dedicated nectarivorous lifestyle and concomitant evolution of bat-dependent pollination (i.e. chiropterophily; see von Helversen, 1993; Winter and von Helversen, 2001; von Helversen and Winter, in press). At biomechanical, behavioral and ecological levels of comparison with hummingbirds, glossophagines thus represent an excellent opportunity to assess convergence in flight physiology and mechanics, as well as to evaluate possible dissimilarities deriving from the phylogenetically disparate origins of these two vertebrate lineages.

To date, the kinematics and mechanics of hovering flight have been examined for only one species of flower bat, *Glossophaga soricina* Pallas (von Helversen, 1986; Norberg et al., 1993). The latter study estimated rather high values for mechanical power expenditure in hovering that substantially exceeded comparable estimates for forward flight at 4.2 m s^{-1}. By contrast, metabolic rates of hovering *G. soricina* exceed those in slow forward flight only by a factor of 20% (Winter, 1998; Winter et al., 1998; Winter and von Helversen, 1998), indicating either that muscle efficiency differs considerably between the two locomotor modes or that expenditure of mechanical power is inadequately understood for this group. Substantial variation in muscle efficiency would be unlikely given the broadly similar wing motions in hovering and forward flight (see Norberg et al., 1993), and the present study thus seeks to investigate further the kinematics and associated mechanical costs of hovering flight in glossophagines.

Also of interest are the allometric limits to hovering flight capacity in vertebrates. Compared with the interspecific range

of body sizes in hummingbirds (mass 2–22 g), glossophagine bats tend to be substantially larger (interspecific range 7–32 g; see Dobat and Peikert-Holle, 1985). The only glossophagine studied thus far in hovering flight, *G. soricina*, is a small species (body mass 9–11 g) on the lower end of the size range exhibited within the subfamily. Given adverse allometric effects on animal flight performance (see Ellington, 1991; Dudley, 2000), we decided to examine both normal hovering and maximum flight capacity for a large glossophagine species (*Leptonycteris curasoae*, the lesser long-nosed bat; mass 23–30 g) that approaches the maximum size within the subfamily. Knowledge of constraints on hovering in this species may thus inform us as to the general nature of body-mass limits on vertebrate flight performance.

To determine limits to hovering flight, we replaced atmospheric nitrogen with helium to create low-density but normoxic flight media that impose novel aerodynamic challenges on volant animals (see Dudley, 1995; Dudley and Chai, 1996). Studies of ruby-throated hummingbirds (*Archilochus colubris*) flying in such hypodense gas mixtures have revealed unexpectedly high reserves of mechanical power, as well as geometrical constraints on stroke amplitude that limit hovering capacity (Chai and Dudley, 1995, 1999). The potential generality of anatomically determined limits to wingbeat kinematics remains to be demonstrated, however, and study of further taxa is warranted. Also, increased oxygen availability does not alter maximum mechanical power output of hummingbirds under hypodense conditions (Chai et al., 1996), and an additional goal of the present research was to assess the effects of supplemental oxygen on hovering flight by glossophagines. We accordingly carried out density-reduction trials under both normoxic and hyperoxic conditions to determine mechanical responses to low and ultimately failure-inducing air densities.

Materials and methods

Experimental animals

Individual *Leptonycteris curasoae* Martinez and Villa were obtained from colonies maintained since 1988 within a large greenhouse at the Institute of Zoology, Erlangen University, Germany. Prior to experiments, bats were maintained in groups of 2–5 individuals within acclimation cages of approximately the same dimensions as the flight chambers used in experiments. Study animals were given access *ad libitum* to a 17% w/w sugar solution (glucose/fructose/sucrose in equal proportions), dilute honey mixtures and a liquid nutritional supplement. Captive animals were subjected to an equatorial light–dark cycle of 12 h/12 h and maintained activity cycles comparable with those of colony bats, albeit within a much smaller flight volume. Weak-flying bats were not used in density-reduction experiments.

Analysis of hover-feeding behavior

Hypodense gas manipulations were carried out inside a large airtight plexiglas cube (1.2 m×1.2 m×1.2 m). A perch within the cube was used by the bats when not flying. Bats fed inside the flight chamber from an artificial nectar feeder supplied externally with a 17% w/w sugar solution. Insertion of the bat's head into the feeder interrupted an infrared light beam and electronically triggered a nectar reward (see Winter et al., 1998). This signal was also used to initiate video recording of hover-feeding sequences (Kappa CF100 camera; 50 fields s^{-1}). The camera was positioned such that the optical axis was orthogonal to one cube face and at the same height as the artificial feeder. The feeder was suspended centrally approximately 50 cm from the ceiling of the cube and was oriented such that bats faced the camera when hover-feeding. A mirror positioned 45° above the experimental chamber was simultaneously filmed by the video camera to record a horizontal projection of wing motions. Partial ambient illumination during experiments was provided by a dim overhead light, whereas video recording was enabled by custom-built stroboscopic infrared flashes positioned outside the cube and driven at repetition rates of 300 Hz. Attached to the feeder at a position just anterior to its opening was an infrared LED, with a corresponding receiver positioned outside of the experimental cube. Wingbeat frequencies of hover-feeding bats were determined from recorded rates of interruption of this infrared light beam by the moving wings, with interruptions occurring once (and sometimes twice) near the bottom of the downstroke. The total duration of each hover-feeding bout was similarly determined from these recordings.

Density-reduction trials

Individual bats were placed within the experimental cube, the gaseous contents of which were then altered through gradual filling with heliox (80% He/20% O_2). Atmospheric nitrogen was thus replaced with helium, while oxygen concentration declined to slightly below the atmospheric value of 20.9%. A small release valve enabled gas replacement during the filling process. Atmospheric pressure, air temperature and relative humidity inside the cube were monitored to enable a precise determination of ambient air density for each trial. At regular intervals, filling with heliox was halted and gas composition within the cube was determined acoustically (see Dudley, 1995). Hover-feeding behavior of the bat was then recorded, an additional density measurement was made, and filling of the cube with heliox was again resumed. This procedure was repeated until an air density was reached at which aerodynamic failure was obtained. Using the same experimental protocol, effects of hyperoxia on maximum hovering performance were determined using a hypodense but hyperoxic gas mixture (65% He/35% O_2); air density declined whereas oxygen concentration increased as this mixture replaced unmanipulated air within the flight chamber.

We defined aerodynamic failure as the inability of the bat to sustain hovering flight for durations typical of those in normodense air, followed by a fluttering descent from the feeder to the floor of the experimental chamber (see also Chai and Dudley, 1995). This latter behavior was never seen in

normodense circumstances and was assumed to indicate the inability of the bat to generate sufficient vertical forces so as to offset body mass. Air density at failure was estimated as the average of the last flight-capable air density and the subsequent air density at which hovering failed. Because air density declined exponentially during the filling process, density intervals became progressively smaller as filling proceeded. Wingbeat kinematics and energetic estimates, however, were determined for the final air density at which hovering flight was sustained. A complete density-reduction trial to the point of aerodynamic failure required 2–3 h; bats typically hung from their perch or, to a much lesser extent, flew around within the cube when not hover-feeding. Experiments were conducted at an average air temperature of 23.8°C (range 23.1–24.7°C) and at an average relative humidity of 74% (range 57–89%).

Determination of morphological and kinematic parameters

Morphological parameters measured on each bat included mean body mass (m) for each experimental trial, wing length (R), total area of both wings (S, excluding the uropatagium) and various wing-shape parameters that were determined following Ellington (1984a). Values for wing loading, p_w ($p_w=mg/S$, where g is gravitational acceleration), and wing aspect ratio, AR ($AR=4R^2/S$), were also calculated.

Wingbeat kinematics were determined from digitization of field-by-field playbacks of recorded video sequences using NIH Image 1.62. Kinematic parameters determined for each hovering sequence included wingbeat frequency (n), stroke plane angle (β), maximum wing positional angle (ϕ_{max}), minimum wing positional angle (ϕ_{min}), mean wing positional angle ($\bar{\phi}$), and stroke amplitude (Φ). Detailed illustrations of these parameters can be found in Ellington (1984b) and Dudley (2000). β was calculated from the two known camera perspectives and from ϕ_{max} and ϕ_{min}. For each hovering sequence, values of wingbeat kinematic parameters were averaged for the right and left wings, whereas, typically, three separate hovering sequences per individual were evaluated at each air density.

Determination of mechanical power expenditure

Kinematic and morphological values were then used in the aerodynamic model of Ellington (1984c) to determine the lift and power requirements of hovering flight. Stroke amplitude, wingbeat frequency, and a number of morphological parameters are used in these calculations. Both the down- and upstroke were assumed to contribute equally to vertical force production (see von Helversen, 1986). Mean lift coefficients were calculated separately for the down- ($C_{L,down}$) and upstrokes ($C_{L,up}$; assuming equal weight support in each half-stroke), whereas a mean Reynolds number (Re) was determined for the entire wingbeat (Ellington, 1984c). Overall power requirements were determined from individual components of profile (P_{pro}), induced (P_{ind}) and inertial (P_{acc}) power. Profile power is the power required to overcome profile drag forces on the wings, whereas induced power is expended in the generation of a downwards momentum flux so as to offset the body mass. Inertial power expenditure varies according to the extent of elastic energy storage of wing inertial energy, the latter being estimated from the wing's mass distribution and its maximum velocity in each of the two half-strokes. A diversity of kinematic and morphological variables thus contributes to these lift and power calculations, for which the work of Ellington (1984a,c) provides further background and details.

Following Norberg *et al.* (1993), a profile drag coefficient of 0.02 was first used to estimate wing profile power. This value derives from steady-state measurements on a hawk wing at Re ranging from approximately 140 000 to 190 000 (see Pennycuick et al., 1992). Values of the Re for wings of hovering glossophagines are substantially lower, however (25,000–40,000; see Table 2), and use of this profile drag coefficient yielded unreasonably high values for the wing lift:drag ratio. Also, recent work on the unsteady aerodynamics of animal wings has revealed higher values for profile drag coefficients than those predicted by steady-state considerations (see Dickinson et al., 1999; Usherwood and Ellington, 2002a,b). No information is available on the drag characteristics of flapping bat wings, although Usherwood and Ellington (2002b) derived maximum lift:drag ratios of approximately 2.0 for a continuously revolving quail wing at an Re of 26 000. Therefore, we also considered a profile drag coefficient of 0.2 in calculations for euglossines, the value of which, when combined with estimated mean lift coefficients for hovering glossophagines (0.6–1.0; see Table 2) yields lift:drag ratios of 3–5. Calculations of wing profile power were made separately for profile drag coefficients of 0.02 and 0.2; this range is likely to encompass actual values.

Inertial power during the first half of a half-stroke was estimated from the moment of inertia of the wings and their maximum angular velocity assuming simple harmonic motion. Wing mass and the associated moment of inertia were estimated from values of body mass using the equation of Thollesson and Norberg (1991). We also included the wing virtual mass in estimates of moment of inertia (Ellington, 1984c; cf. Norberg et al., 1993). Because of partial wing flexion during the upstroke, the total moment of inertia during this half-stroke was assumed to equal 50% of the downstroke value (Norberg et al., 1993). Total body-mass-specific power requirements were calculated for the two cases of perfect (P_{per}) and zero (P_{zero}) elastic energy storage of wing inertial energy (Ellington, 1984c). In order to estimate muscle-mass-specific power output, one male bat was euthanized by cervical dislocation for postmortem measurement of flight muscle mass. For this individual, the major down- and upstroke muscles represented 26% of total body mass (27.1 g). This value was used here as representative for all individuals to provide a first-order estimate of muscle-mass-specific power output in hovering flight.

Statistical analysis

Two-way analysis of variance (ANOVA) was used to

Table 1. *Morphological parameters, failure density and mean hovering duration at failure for five glossophagine bats in normoxic and hyperoxic density-reduction trials*

ID#/gender	Treatment	m (g)	R (mm)	$\mathcal{AR}$	p_w (N m^{-2})	ρ_f (kg m^{-3})	t (s)
1/M	Normoxia	27.55	160.6	5.74	15.03	0.685	0.611
2/F	Normoxia	27.15	159.3	5.18	13.58	0.715	0.292
	Hyperoxia	27.63	159.3	5.18	13.82	0.681	0.230
3/M	Normoxia	23.60	158.2	5.43	12.53	0.676	0.336
4/M	Normoxia	25.43	168.6	6.47	14.18	0.618	0.493
	Hyperoxia	24.96	168.6	6.47	13.92	0.600	0.695
5/M	Normoxia	25.52	160.7	5.89	14.25	0.635	0.861
	Hyperoxia	25.48	160.7	5.89	14.23	0.650	0.253
	Normoxia (mean)	25.85	161.5	5.74	13.91	0.666	0.519
	Hyperoxia (mean)	26.02	162.9	5.85	13.99	0.643	0.393

Abbreviations: ID#, bat identification number; m, body mass for each experiment; R, wing length; $\mathcal{AR}$, wing aspect ratio; p_w, wing loading; ρ_f, air density at failure; estimated as the average of the last flight-capable air density and the subsequent air density at which hovering was unsuccessful); t, mean hovering duration at the last flight-capable air density.

evaluate the effects of air density and oxygen availability on kinematic, aerodynamic and energetic variables; air densities were pooled into 0.1 kg m^{-3} intervals to yield a categorical density variable for this statistical analysis.

Results

Five individual bats were flown to failure in normoxic density-reduction trials; failure in hovering for three of these five bats was also evaluated in hyperoxic heliox-air mixtures (Table 1). Behaviorally, bats became more reluctant to fly as air density was reduced, often tenaciously holding onto their perch near the failure density. When leaving the feeder at near-failure air densities, bats would typically descend a considerable distance before then ascending to the perch, a behavior not seen under normodense conditions. The air density at failure in normoxia averaged 0.67 kg m^{-3} (see Table 1).

Hovering duration at the air density immediately prior to failure averaged 0.5 s and did not vary significantly with air density (Tables 1, 4). Of measured wingbeat kinematic parameters, stroke amplitude (Φ) and its constituent parameters of maximum (ϕ_{max}) and minimum (ϕ_{min}) wing positional angle showed systematic change with reduced air density (Tables 2, 4; see also Fig. 1). Stroke amplitude increased on average by 26% at the near-failure density, reflecting average increases of 20% in ϕ_{max} and of 31% in ϕ_{min}. Both mean positional angle ($\bar{\phi}$) of the wings in the stroke plane and the wingbeat frequency (n) showed slight but non-significant decreases in hypodense air (Table 4). Although stroke amplitude, and thus mean wingtip velocity (given constant flapping frequency), increased following heliox infusion, mean Re of the wings decreased significantly (P<0.001, N=5) as a consequence of the relatively larger decline in air density (see Tables 2, 4). Mean lift coefficients (C_L), however, showed no systematic change with air density (Tables 2, 4).

In normodense air, estimates of profile power (P_{pro}) ranged from 2.9 W kg^{-1} body mass to 29.0 W kg^{-1} body mass, depending on the assumed profile drag coefficient (Table 3). Profile power thus ranged from 14% to 63% of the aerodynamic power expenditure; the sum of the induced and profile powers (see Table 3, Fig. 2). Inertial power expended during the first half of a half-stroke (P_{acc}) typically exceeded aerodynamic power by a factor of four to five. Assuming perfect elastic storage of wing inertial energy and a profile drag coefficient of 0.02, total power expenditure (P_{per}) in normodense hovering averaged 20.1 W kg^{-1} body mass

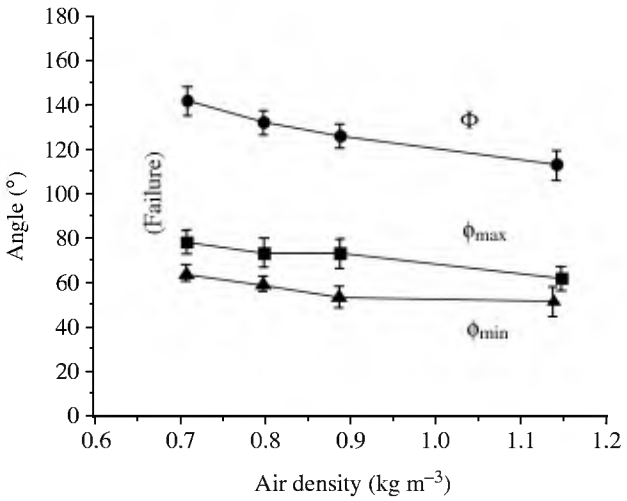

Fig. 1. Maximum wing positional angle ϕ_{max}, minimum wing positional angle ϕ_{min}, and total stroke amplitude Φ as a function of air density in normoxic density-reduction trials. Error bars indicate 1 S.D. (N=5 individuals).

Table 2. *Mean values of air density, kinematic, aerodynamic variables in normodense hovering and immediately prior to hypodense hovering failure under both normoxic and hyperoxic conditions*

	ρ (kg m^{-3})	n (Hz)	Φ (°)	β (°)	ϕ_{max} (°)	ϕ_{min} (°)	$\bar{\phi}$ (°)	$C_{L,down}$	$C_{L,up}$	Re
Normoxia										
Normodense hovering										
Mean (N=5)	1.14	11.7	112.6	47.0	51.2	–61.4	–5.1	0.82	0.67	37800
S.D.	0.01	0.9	15.4	2.8	10.5	12.7	8.8	0.23	0.17	7470
Near-failure										
Mean (N=5)	0.72	11.3	141.6	44.0	61.4	–80.2	–9.4	1.00	0.84	24960
S.D.	0.04	0.97	16.9	4.0	12.5	8.2	6.4	0.47	0.33	4490
Hyperoxia										
Normodense hovering										
Mean (N=3)	1.13	11.3	108.8	51.4	46.7	–62.1	–7.7	0.76	0.63	38150
S.D.	0.00	0.48	19.0	6.9	11.6	12.0	7.0	0.20	0.15	5710
Near-failure										
Mean (N=3)	0.70	11.2	138.0	49.2	55.6	–82.4	–13.4	0.74	0.64	32600
S.D.	0.06	0.78	18.0	7.8	11.3	10.3	5.9	0.28	0.23	11370

Abbreviations: n, wingbeat frequency; Φ, stroke amplitude; β, stroke plane angle; ϕ_{max}, maximum wing positional angle; ϕ_{min}, minimum wing positional angle; $\bar{\phi}$, mean positional angle; $C_{L,down}$, mean lift coefficient during downstroke; $C_{L,up}$, mean lift coefficient during upstroke; Re, mean Reynolds number.

Table 3. *Mean values of body mass-specific power variables in normodense hovering and immediately prior to hypodense hovering failure under normoxic and hyperoxic conditions*

	P_{ind} (W kg^{-1})	P_{pro} (W kg^{-1})	P_{acc} (W kg^{-1})	P_{per} (W kg^{-1})	P_{zero} (W kg^{-1})
Normoxia					
Normodense hovering					
Mean (N=5)	17.2	2.9 (29.0)	99.2	20.1 (31.9)	59.7 (72.7)
S.D.	1.3	1.4 (14.5)	39.6	1.5 (16.0)	19.4 (27.7)
Near-failure					
Mean (N=5)	19.5	4.1 (41.3)	102.3	23.6 (45.4)	63.0 (81.5)
S.D.	1.3	2.0 (19.6)	35.1	1.6 (21.6)	20.7 (28.0)
Hyperoxia					
Normodense hovering					
Mean (N=3)	17.7	3.1 (30.5)	98.2	20.7 (33.5)	59.5 (73.2)
S.D.	1.6	1.0 (9.6)	26.5	1.9 (10.6)	16.3 (18.9)
Near-failure					
Mean (N=3)	18.6	4.0 (39.7)	22.5	22.5 (43.7)	71.7 (89.6)
S.D.	2.1	1.8 (17.5)	2.4	2.4 (19.3)	19.6 (26.3)

Abbreviations: P_{ind}, body mass-specific induced power; P_{pro}, body mass-specific profile power; P_{acc}, body mass-specific inertial power during first half of a half-stroke; and body mass-specific mechanical power output assuming perfect (P_{per}) and zero (P_{zero}) elastic storage of wing inertial energy.

Values of P_{pro}, P_{per} and P_{zero} refer to calculations with a profile drag coefficient of 0.02; numbers in parentheses refer to a profile drag coefficient of 0.2 (see text).

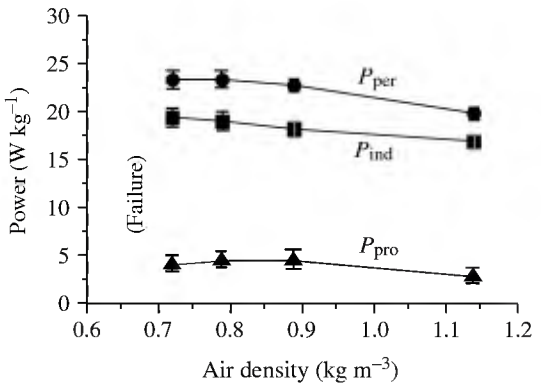

Fig. 2. Body-mass-specific induced power (P_{ind}), profile power (P_{pro}) and total power requirements assuming perfect elastic energy storage (P_{per}) as a function of air density in normoxic density-reduction trials. Error bars indicate 1 S.D. (N=5 individuals). Values of P_{pro} and P_{per} derive from an assumed profile drag coefficient of 0.02 (see text).

(Fig. 2), yielding a value of 77.3 W kg^{-1} muscle mass given a relative flight muscle mass of 26%. The corresponding values for a profile drag coefficient of 0.2 were 31.9 W kg^{-1} body mass and 122.7 W kg^{-1} muscle mass. At near-failure air densities, induced power expenditure (P_{ind}) was 14% greater than in normodense air, whereas the associated increase in P_{pro} was approximately 42% (Table 3). Again, assuming perfect elastic energy storage, a profile drag coefficient of either 0.02 or 0.2 and a flight muscle ratio of 26%, the muscle-mass-specific power output at the point of near-failure was either 90.8 W kg^{-1} or 175.6 W kg^{-1}, an increase of either 17% or 43%, respectively, relative to normodense hovering. At both normal and near-failure air densities, total power requirements assuming zero elastic energy storage of wing inertial energy (P_{zero}) were substantially greater than the aerodynamic power requirements alone (Table 3).

In hyperoxic density-reduction trials, stroke plane angles (β) increased significantly (P<0.001, N=5) at lower air densities, by approximately 10% on average (Tables 2, 4). No other kinematic or energetic variable changed systematically with increased oxygen availability. Also, none of the potential interaction effects between air density and oxygen treatment were significant. At the point of aerodynamic failure in hypodense hyperoxia, oxygen concentration was estimated to be approximately 33%. Near-failure air densities in hyperoxia did not differ significantly from those obtained for normoxic density reduction (unpaired t-test, t=1.05, P>0.30; see also Table 4).

Table 4. *Results of analysis of variance (ANOVA) for kinematic and mechanical variables in density-reduction trials under two conditions of oxygen availability (normoxia and hyperoxia)*

	F value		
Variable	Density	Oxygen	Density/ oxygen interaction
n	1.16	2.21	0.32
t	0.08	0.08	0.94
Φ	11.56***	0.20	0.43
β	1.18	10.46***	1.82
ϕ_{max}	4.04**	0.47	0.31
ϕ_{min}	7.55***	0.01	0.70
ϕ	0.93	0.30	0.53
$C_{L,down}$	0.17	3.67	0.77
$C_{L,up}$	1.95	3.42	0.86
Re	11.0***	3.28	0.73
P_{ind}	6.99***	0.19	1.33
P_{pro}	2.65*	0.18	1.24
P_{acc}	2.21	1.58	0.42
P_{per}	9.13***	0.01	3.22
P_{zero}	2.42	1.53	0.44

P values (*P<0.05, **P< 0.01, ***P<0.001) are from F test; degrees of freedom are (4,99) for the density treatment, (1,99) for the oxygen treament, and (4,99) for the density/oxygen interaction.

Symbols are defined in Tables 2 and 3. Values of P_{pro}, P_{per} and P_{zero} in this ANOVA were derived using a profile drag coefficient of 0.02, but the overall statistical results were unchanged by use of the higher coefficient of 0.2.

Discussion

Air densities at which *L. curasoae* could not sustain flight were substantially below the normodense value and did not change in hyperoxia. Hovering duration at the feeder was independent of air density, possibly because a reduction in hovering time below the already short value typical of normodense conditions (approximately 500 ms) would be insufficient for nectar extraction. As with hummingbirds hovering in hypodense air (Chai and Dudley, 1995, 1996), kinematic responses of *L. curasoae* to hypodense aerodynamic challenge involved increases in stroke amplitude but maintenance of a constant wingbeat frequency. Stroke amplitude increased by approximately 26% prior to failure, whereas a much smaller reserve characterized mechanical power output (i.e. a 5–20% increase; see Table 3). Mean lift coefficients did not vary systematically with air density, but this result may partly derive from the high variance exhibited among individuals for this derived variable (see Table 2). In contrast to results for hummingbirds (Chai and Dudley, 1995), stroke amplitude of glossophagines at the point of aerodynamic failure did not approach 180° but rather averaged a much lower 142° (Table 2). Whether this value corresponds to a true anatomical constraint on wingbeat kinematics or instead represents the point at which power output becomes limiting is unclear (see below).

For glossophagines generally, the kinematic and energetic reserves induced by low-density aerodynamic challenge are unlikely to derive from adaptations for flight under conditions of natural hypobaria. In contrast to the often montane and even high-altitude habitats of many hummingbirds, flower bats tend to be found at low- to mid-elevations, except for some species in the genus *Anoura*, which can be found up to 3400 m (F. Matt, personal communication). *L. curasoae* is predominantly a lowland species, although a night roost has been recorded at an elevation of 1240 m (Herrera Montalvo, 1997; see also Reid, 1997). By contrast, the average air density at failure for *L. curasoae* corresponds to an altitude of approximately 3000 m. The capacity of this species to sustain hovering under hypodense but normobaric conditions probably derives from the need in normodense air for supplemental power in vertical-ascent, climbing flight or for translational accelerations and fast forward flight. Female glossophagines are confronted by the additional need to carry their young both pre- and postnatally, increasing their effective mass by approximately 30% and entailing substantial energetic costs (see Voigt, 2000).

Some of the aerodynamic assumptions used here should be considered provisional, although the overall conclusions are probably robust. The extent to which force partitioning between half-strokes changes with increased aerodynamic requirements is unclear given the complexities of tip reversal and variable upstroke geometry in glossophagines. Substantial longitudinal wing flexion during the upstroke also suggests considerable deviation of wingtip motions from simple harmonic motion. Following Norberg et al. (1993), and in the absence of high-speed kinematic analysis for *L. curasoae*, we here assumed equal durations for the down- and upstroke. Aerodynamically, the assumption of a constant profile drag coefficient is also probably inappropriate for the range of Reynolds numbers exhibited during density-reduction trials. Our estimates of aerodynamic power based on two extremes for the profile drag coefficient probably bracket actual values, although we emphasize the present ignorance of profile drag data for reciprocating vertebrate appendages. As with all flying vertebrates, the actual extent of elastic energy storage within the flight apparatus is unknown, although potential sites for such storage include flight muscle, tendons, wing bones and even the wing membrane itself. Costs of flight in the absence of such storage will increase substantially (Table 3).

Norberg et al. (1993) estimated induced and profile powers for hovering and slow forward flight ($4.2\,m\,s^{-1}$) of the glossophagine *G. soricina*. Calculations of instantaneous inertial torque were then compared with estimated aerodynamic torque at different wing positions to determine potential inertial contributions to aerodynamic work. As noted by Ellington (1984c), this approach presupposes accurate calculation of wing accelerations from wing positional information, a procedure potentially subject to error. Instead, mean values of wing inertial energy can be estimated for the first half of a half-stroke, as was done in the present study. If all such energy is stored elastically, then total power over the half-stroke is the aerodynamic power alone. In the absence of such storage, total power equals half the sum of the inertial power and the aerodynamic power (Ellington, 1984c). Reanalyzing the power values of Norberg et al. (1993) in this way yields a body-mass-specific power expenditure of $14.9\,W\,kg^{-1}$ for the case of perfect elastic energy storage and a profile drag coefficient of 0.02, as used in the original paper. This value may be compared with a similarly modified estimate of $8.7\,W\,kg^{-1}$ body mass based on data provided in the same paper for a different individual of *G. soricina* in slow forward flight. The original estimates of Norberg et al. (1993) are $32.4\,W\,kg^{-1}$ for hovering and $12.3\,W\,kg^{-1}$ for forward flight, the ratio of which quantities is substantially higher than the corresponding ratio for the above modified estimates. Note, however, that wingbeat frequencies of the two individual bats used in this comparison were also substantially different (i.e. 15.2 Hz in hovering *versus* 11.8 Hz in forward flight), which would yield a reduced profile power in forward flight and thus underestimate total costs. Detailed kinematic data for individual glossophagines in both hovering and in slow forward flight are unfortunately not available, although existing metabolic data suggest that the costs of flight are broadly similar for these two modes of locomotion (see Winter, 1998; Winter and von Helversen, 1998; Winter et al., 1998; Voigt and Winter, 1999). In summary, the previously reported differences between hovering and forward flight in glossophagines are probably overestimated, but particularly our understanding of unsteady profile drag force on bat wings precludes a more detailed energetic analysis at present.

The estimate of maximum power output in *L. curasoae* varied between $91\,W\,kg^{-1}$ muscle and $176\,W\,kg^{-1}$ muscle, assuming perfect elastic energy storage of wing inertial energy and a likely range of profile drag coefficients. If power output is not equally distributed between down- and upstrokes, as assumed here, then average power output during the downstroke may be much higher. By comparison, ruby-throated hummingbirds in hypodense but normoxic gas mixtures fail to sustain hovering at muscle-mass-specific power outputs of approximately $140\,W\,kg^{-1}$ (Chai and Dudley, 1995, 1996). This failure is associated with a geometrical constraint on stroke amplitude and is unaffected by an increased oxygen partial pressure (Chai et al., 1996). In glossophagines, hyperoxia similarly fails to enhance hovering performance (ruling out diffusive constraints on power availability), but stroke amplitudes are well below limiting values for hummingbirds in heliox. Does an anatomical constraint pertain for *L. curasoae* or are there additional kinematic and power reserves that may be exhibited in different behavioral contexts of flight? Compared with ruby-throated hummingbirds, the large bats in the present study exhibited a much smaller relative increase in power output with respect to hovering in normodense air. Maximum stroke amplitude in this case may simply yield the maximum power output available from the muscle. An additional approach to this issue for glossophagines would be to carry out load-lifting experiments (Chai et al., 1997) that evaluate the ability to sustain loads vertically during hovering. For ruby-throated

hummingbirds, such experiments have shown short-duration but high-intensity power outputs (approximately 200 W kg^{-1} muscle) that exceed by 50% the maxima found in density-reduction trials (Chai et al., 1997). Stroke amplitudes or power outputs significantly in excess of those exhibited in hypodense air would further illustrate context-dependence of the limits to flight performance. Physical manipulation of glossophagine wings on live animals suggests that maximum positional angles well in excess of those attained in heliox (i.e. >61°; see Table 2) can be attained anatomically but have not been documented for free-flying bats.

Comparison of hovering energetics between hummingbirds and glossophagines indicates lower flight costs in the latter taxon because of their much higher wing surface area relative to body mass (Voigt and Winter, 1999). Wing loading is accordingly much lower in glossophagines, and induced power costs are correspondingly reduced. In part, such morphological differences may explain why large glossophagines substantially exceed the largest hummingbird species in terms of body mass. A relative reduction in mechanical power expenditure for the former taxon may simply permit an increased body size up to the point of a mechanical power limitation. Hovering data for the largest hummingbird species (*Patagona gigas*) are not currrently available, but, if power limits generally pertain to vertebrate hovering performance, we might expect comparable maximum mechanical power output between this hummingbird and the largest glossophagines.

Alternatively, flight muscle efficiencies may differ substantially between the two taxa for phylogenetic reasons, although calculations using available data suggest that this is not the case. For an average *L. curasoae* weighing 26 g (Table 1), the scaling of power input given by Voigt and Winter (1999) for glossophagines predicts a body-mass-specific metabolic rate in hovering of 154 W kg^{-1}. Assuming perfect elastic energy storage, this value can be combined with the average values determined here for mechanical power output (20.1 W kg^{-1} body mass and 31.9 W kg^{-1} body mass; Table 3) to yield muscle efficiencies between 13% and 21%. This value is somewhat higher than that derived for ruby-throated hummingbirds in normal hovering flight (10–11%; see Chai and Dudley, 1995, 1996), but these latter estimates were made prior to the aforementioned upwards revisions in unsteady profile drag coefficients and may thus be substantial underestimates of total power. Also, maximum metabolic power input at the point of hypodense failure in ruby-throated hummingbirds averages 307 W kg^{-1}, but muscle efficiencies are unchanged relative to normodense hovering (Chai and Dudley, 1995, 1996). We emphasize, however, that metabolic rates in hovering *L. curasoae* have not yet been measured under either normodense or near-failure hypodense conditions. In particular, the equation of Voigt and Winter (1999) is derived from data for three glossophagine species, all of which are below 20 g in body mass.

Hovering, and more generally the ability to generate vertical forces during flight, represents only one component of flight maneuverability, namely force production along one of the three orthogonal body axes. Other features of flight performance involving axial force production (e.g. thrust generation during forward flight), as well as various components of torsional agility (i.e. the rapidity of body rotations about each of three orthogonal axes), are equally important features of animal flight (see Dudley, 2002). Features of body design conducive to performance in one context may be limiting in other modes of flight. In ruby-throated hummingbirds, for example, sexually dimorphic morphological features yield strong differences in maximum hovering performance, but maximum flight speeds are equivalent between the sexes (Chai and Dudley, 1999; Chai et al., 1999). Little is known about forward flight performance in *L. curasoae*, although the long-distance commuting flight of this species in nature occurs at airspeeds close to 8 m s^{-1} (Sahley et al., 1993). Such speeds are likely to exceed the slow forward flight mentioned previously and may well lie on the ascending portion of the 'U'-shaped power curve proposed by Voigt and Winter (1999) as characteristic for bats weighing >6–7 g.

As with hummingbirds, hovering in glossophagines is of monophyletic origin and is confined to the New World. Most nectarivorous fruit bats land on rather than hover at flowers (Dobat and Peikert-Holle, 1985). However, Gould (1978) observed hovering of a small macroglossine pteropodid in front of flowers prior to landing (see also Strahan, 1983). Transient hovering has been reported for a number of other bat taxa (see Norberg and Rayner, 1987), and Voigt and von Helversen (1999) observed a hovering display flight of 17 s duration in the emballonurid *Saccopteryx bilineata*. Nonetheless, glossophagines effect stable hovering with apparently little force asymmetry between the down- and upstrokes, although quantitative partitioning of weight support between the two half-strokes remains unknown. Such hovering abilities are even more remarkable given the limited (but distal) wing reversal described for the glossophagine upstroke (von Helversen, 1986). Morphological features of flower bats associated with hovering include rounded wingtips, relatively long third digits and high wingtip (chiropatagial) areas (see Smith and Starrett, 1979; Norberg and Rayner, 1987).

Given that sustained hovering is a behavioral novelty that originated only twice among volant vertebrates, evolutionary study of the kinematics and mechanics of hovering behavior among phyllostomids would be of substantial interest. Recent phylogenetic analyses suggest that predominant nectarivory arose once within the Phyllostomidae, although occasional nectar-feeding characterizes a number of other lineages within the family (see Ferrarezzi and Gimenez, 1996; Wetterer et al., 2000). We do not know, however, which and to what degree flight-related features have changed in concert with such dietary specialization. Of particular interest would be a comparison of glossophagine flight performance with that of closely related phyllostomid taxa such as the phyllonycterines and the brachyphillines that occasionally feed on nectar. Dedicated nectarivory has also been associated in phyllostomids with substantial shifts in digestive and renal function (Schondube et

al., 2001). As with hummingbirds (Altshuler and Dudley, 2002), biomechanical and physiological origins of the hovering lifestyle in glossophagines remain obscure. Future studies mapping morphological and kinematic features of hovering flight onto a well-resolved phyllostomid phylogeny should resolve such uncertainties.

We thank Doug Altshuler, Brendan Borrell, Ryan Hill, Travis LaDuc, Otto von Helversen and two anonymous reviewers for useful comments, and the Deutsche Forschungsgemeinschaft, the German Academic Exchange Service and the U.S. National Science Foundation (IBN-9817138) for research support.

References

Altshuler, D. and Dudley, R. (2002). The ecological and evolutionary interface of hummingbird flight physiology. *J. Exp. Biol.* **205**, 2325-2336.

Chai, P., Altshuler, D. L., Stephens, D. B. and Dillon, M. E. (1999). Maximal horizontal flight performance of hummingbirds: effects of body mass and molt. *Physiol. Biochem. Zool.* **72**, 145-155.

Chai, P., Chen, J. S. C. and Dudley, R. (1997). Transient hovering performance of hummingbirds under conditions of maximal loading. *J. Exp. Biol.* **200**, 921-929.

Chai, P. and Dudley, R. (1995). Limits to vertebrate locomotor energetics suggested by hummingbirds hovering in heliox. *Nature* **377**, 722-725.

Chai, P. and Dudley, R. (1996). Limits to flight energetics of hummingbirds hovering in hypodense and hypoxic gas mixtures. *J. Exp. Biol.* **199**, 2285-2295.

Chai, P. and Dudley, R. (1999). Maximum flight performance of hummingbirds: capacities, constraints, and trade-offs. *Am. Nat.* **153**, 398-411.

Chai, P., Harrykissoon, R. and Dudley, R. (1996). Hummingbird hovering performance in hyperoxic heliox: effects of body mass and sex. *J. Exp. Biol.* **199**, 2745-2755.

Dobat, K. and Peikert-Holle, T. (1985). *Blüten und Fledermäuse (Chiropterophilie)*. Frankfurt: Kramer Verlag.

Dickinson, M. H., Lehmann, F. O. and Sane, S. P. (1999). Wing rotation and the aerodynamic basis of insect flight. *Science* **84**, 1954-1960.

Dudley, R. (1995). Extraordinary flight performance of orchid bees (Apidae: Euglossini) hovering in heliox (80% He/20% O_2). *J. Exp. Biol.* **198**, 1065-1070.

Dudley, R. (2000). *The Biomechanics of Insect Flight: Form, Function, Evolution*. Princeton: Princeton University Press.

Dudley, R. (2002). Mechanisms and implications of animal flight maneuverability. *Integr. Comp. Biol.* **42**, 135-140.

Dudley, R. and Chai, P. (1996). Animal flight mechanics in physically variable gas mixtures. *J. Exp. Biol.* **199**, 1881-1885.

Ellington, C. P. (1984a). The aerodynamics of hovering insect flight. II. Morphological parameters. *Phil. Trans. R. Soc. Lond. B* **305**, 17-40.

Ellington, C. P. (1984b). The aerodynamics of hovering insect flight. III. Kinematics. *Phil. Trans. R. Soc. Lond. B* **305**, 41-78.

Ellington, C. P. (1984c). The aerodynamics of hovering insect flight. VI. Lift and power requirements. *Phil. Trans. R. Soc. Lond.* B **305**, 145-181.

Ellington, C. P. (1991). Limitations on animal flight performance. *J. Exp. Biol.* **160**, 71-91.

Ferrarezzi, H. and Gimenez, E. A. (1996). Systematic patterns and the evolution of feeding habits in Chiroptera (Archonta: Mammalia). *J. Comp. Biol.* **1**, 75-94.

Gould, E. (1978). Foraging behavior of Malaysian nectar-feeding bats. *Biotropica* **10**, 184-193.

Herrera Montalvo, L. G. (1997). Evidence of altitudinal movements of *Leptonycteris curasoae* (Chiroptera: Phyllostomidae) in central Mexico. *Rev. Mex. Mastozool.* **2**, 116-118.

Norberg, U. M. (1990). *Vertebrate Flight*. Berlin: Springer-Verlag.

Norberg, U. M., Kunz, T. H., Steffensen, J. F., Winter, Y. and von Helversen, O. (1993). The cost of hovering and forward flight in a nectar-feeding bat, *Glossophaga soricina*, estimated from aerodynamic theory. *J. Exp. Biol.* **182**, 207-227.

Norberg, U. M. and Rayner, J. M. V. (1987). Ecological morphology and flight in bats (Mammalia: Chiroptera): wing adaptations, flight performance, foraging strategy and echolocation. *Phil. Trans. R. Soc. Lond. B* **316**, 335-427.

Pennycuick, C. J., Heine, C. E., Kirkpatrick, S. J. and Fuller, M. R. (1992). The profile drag of a hawk's wing, measured by wake sampling in a wind tunnel. *J. Exp. Biol.* **165**, 1-19.

Reid, F. A. (1997). *A Field Guide to the Mammals of Central America and Southeast Mexico*. Oxford: Oxford University Press.

Sahley, C. T., Horner, M. A. and Fleming, T. H. (1993). Flight speeds and mechanical power outputs of the nectar-feeding bat, *Leptonycteris curasoae* (Phyllostomidae: Glossophaginae). *J. Mamm.* **74**, 594-600.

Schondube, J. E., Herrera, L. G. and Martínez del Rio, C. (2001). Diet and the evolution of digestion and renal function in phyllostomid bats. *Zoology* **104**, 59-73.

Smith, J. D. and Starrett, A. (1979). Morphometric analysis of chiropteran wings. In *Biology of Bats of the New World Family Phyllostomidae*, vol. 3 (ed. R. J. Baker, J. K. Jones and D. C. Carter), pp. 427-437. Lubbock, TX: Texas Tech University.

Strahan, R. E. (1983). *The Australian Museum Complete Book of Australian Mammals*. Sydney: Angus & Robertson.

Thollesson, M. and Norberg, U. M. (1991). Moments of inertia of bat wings and body. *J. Exp. Biol.* **158**, 19-35.

Usherwood, J. R. and Ellington, C. P. (2002a). The aerodynamics of revolving wings. I. Model hawkmoth wings. *J. Exp. Biol.* **205**, 1547-1564.

Usherwood, J. R. and Ellington, C. P. (2002b). The aerodynamics of revolving wings. II. Propeller force coefficients from mayfly to quail. *J. Exp. Biol.* **205**, 1565-1576.

Voigt, C. C. (2000). Intraspecific scaling of flight power in the bat *Glossophaga soricina*. *J. Comp. Physiol. B* **170**, 403-410.

Voigt C. C. and von Helversen, O. (1999). Storage and display of odor in male *Saccopteryx bilineata* (Chiroptera, Emballonuridae). *Behav. Ecol. Sociobiol.* **47**, 29-40.

Voigt, C. C. and Winter, Y. (1999). Energetic cost of hovering flight in nectar-feeding bats (Phyllostomidae: Glossophaginae) and its scaling in moths, birds and bats. *J. Comp. Physiol. B* **169**, 38-48.

von Helversen, O. (1986). Blü tenbesuch bei Blumenfledermäusen: Kinematik des Schwirrfluges und Energiebudget im Freiland. In *Biona-report 5: Fledermausflug-bat flight* (ed. W. Nachtigall), pp. 107-126. Stuttgart: G. Fischer.

von Helversen, O. (1993). Adaptations of flowers to the pollination by glossophagine bats. In *Animal–Plant Interactions in Tropical Environments* (ed. W. Barthlott), pp. 41-59. Bonn: Museum Koenig.

von Helversen, O. and Winter, Y. Glossophagine bats and their flowers: cost and benefit for plant and pollinator. In *Ecology of Bats* (ed. T. H. Kunz and M. B. Fenton). Chicago: University of Chicago Press. In press.

Wetterer, A. L., Rockman, M. V. and Simmons, N. B. (2000). Phylogeny of phyllostomid bats (Mammalia: Chiroptera): data from diverse morphological systems, sex chromosomes, and restriction sites. *Bull. Am. Mus. Nat Hist.* **248**, 1-200.

Winter, Y. (1998). Energetic cost of hovering flight in a nectar-feeding bat measured with fast-response respirometry. *J. Comp. Physiol. B* **168**, 434-444.

Winter, Y. and von Helversen, O. (1998). The energy cost of flight: do small bats fly more cheaply than birds? *J. Comp. Physiol. B* **168**, 105-111.

Winter, Y. and von Helversen, O. (2001). Bats as pollinators: foraging energetics and floral adaptations. In *Cognitive Ecology of Pollination* (ed. L. Chittka and J. Thomson), pp. 148-170. Cambridge: Cambridge University Press.

Winter, Y., Voigt, C. and von Helversen, O. (1998). Gas exchange during hovering flight in a nectar-feeding bat *Glossophaga soricina*. *J. Exp. Biol.* **201**, 237-244.